ARTICLE

Fabrication of PbS Quantum Dot Doped TiO_2 Nanotubes

Chalita Ratanatawanate, Chunrong Xiong, and Kenneth J. Balkus, Jr.*

Department of Chemistry and the Alan G. MacDiarmid NanoTech Institute, The University of Texas at Dallas, Richardson, Texas 75083-0688

ABSTRACT PbS quantum dots (PbS QDs) were prepared on the inside and outside surfaces of TiO_2 nanotubes by using thiolactic acid as an organic linker. The sizes of PbS QDs were controlled by employing a dip coating process to anchor the PbS QDs onto the TiO_2 nanotubes. The PbS QDs with diameters of 2−10 nm were obtained by adjusting the concentration of thiolactic acid. TiO_2 nanotubes with PbS QDs located only inside the nanotubes were prepared by first coating the tubes with the double-chain cationic surfactant DDAB. The PbS QDs supported on TiO_2 nanotubes were characterized by TEM, as well as Raman, FT-IR, and UV−vis spectroscopy.

KEYWORDS: PbS · quantum dots · TiO_2 · nanotubes · tunable band gap

Many applications that exploit free energy from the sun, including converting sunlight to electricity (solar cell), transforming energy from the sun to generate fuel (water splitting), and degrading the toxic chemicals to environmental friendly compounds (photodegradation of organic compounds), continue to grow in importance.[1−3] The surface photochemistry as well as physical and chemical stability of the semiconductor, TiO_2, makes it an attractive material for these applications. Unfortunately, TiO_2 (anatase) has a large band gap (3.2 eV), which is too large for efficient absorption of energy from sunlight. Therefore, much effort has been devoted to modifying the band gap of TiO_2 to improve the overlap of the absorption spectrum with the solar spectrum. One strategy is to combine TiO_2 with a semiconductor that has a narrow band gap and an energetically high-lying conduction band.[4] Lead sulfide (PbS) is a good candidate because of its small band gap (0.41 eV) and its large exciton Bohr radius of 20 nm, which leads to extensive quantum size effects.[5] PbS quantum dots (PbS QDs) are expected to further improve photocatalytic activity of TiO_2 due to multiple exciton generation (MEG) and efficient spatial separation of photogenerated charge, preventing electron−hole recombination.[6,7] It has been reported that the absorption range can be tuned by adjusting the particle size of the quantum dots.[8] Hence, various studies have been focused on development of the methods for synthesis of the controllable size PbS QDs. For example, some of these include synthesis in colloidal solutions,[9] reverse micelles and microemulsions,[10] and matrix supports (polymers, block copolymers, and sol−gel matrixes) to stabilize the nanoparticles.[11−13] The fabrication of TiO_2 supported PbS has also been reported. For example, Hoyer and Könenkamp prepared PbS doped TiO_2 films by dipping the TiO_2 film into a concentrated lead acetate solution and subsequently precipitating the absorbed Pb^{2+} with sodium sulfide solution to yield 3 nm PbS QDs.[14] Sun and co-workers prepared PbS coupled TiO_2 colloid by using mercaptoacetic acid as bridging units with the carboxyl groups anchored to the TiO_2 surfaces and thiol groups

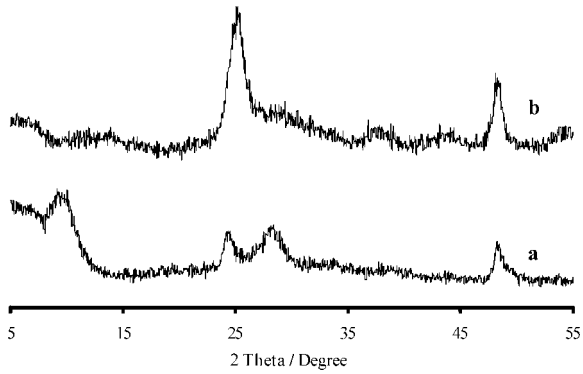

Figure 1. XRD patterns of TiO_2 nanotubes after acid washing, (a) before and (b) after annealing at 350 °C, respectively.

*Address correspondence to balkus@utdallas.edu.

Received for review March 7, 2008 and accepted June 02, 2008.

Published online August 6, 2008. 10.1021/nn800141e CCC: $40.75

binding with Pb^{2+}.[15] Yang *et al.* and collaborators modified a TiO_2 electrode with PbS QDs by chemical deposition.[16] Plass *et al.* used a chemical bath deposition technique to attach PbS QDs onto a mesoporous TiO_2 substrate.[17] Using the similar sequential chemical bath deposition process, Sun and co-workers fabricated a CdS QD sensitized nanotube array photoelectrode. They reported that the generated photocurrent response of the QD sensitized TiO_2 electrode achieved was 35 times higher than that of the bare TiO_2 nanotube electrode.[18]

In this study, TiO_2 nanotubes (TNTs) were selected as a support since 1D TNTs afford a high surface-to-volume ratio and tunable electron transport properties due to quantum confinement effects, yielding enhanced catalytic activity.[19] Additionally, it may be possible to control the PbS QD size by encapsulation inside the TNTs' pores which have a fixed diameter. Here, we have employed a dip coating process to decorate the TNTs with PbS QDs. To prevent the formation of bulk PbS, the TiO_2 surfaces were first treated with thiolactic acid which provides a binding site for Pb^{2+} ions. Since the amount of thiolactic acid linker determines the amount of Pb^{2+} ions that are bonded to the TNTs, the amount of thiolactic acid indirectly determines the size of the QDs. Thus, PbS QDs with controllable size were made onto the TiO_2 surfaces by reacting Na_2S with the Pb^{2+} ions, absorbed on the pretreated surfaces. By adjusting the concentration of thiolactic acid, PbS QDs with 2−10 nm were obtained. Moreover, we have developed a method to place PbS QDs only in the inside TNTs by blocking the outer surface with surfactant before impregnation with PbS QDs. The TiO_2 nanotube supported PbS quantum dots were characterized by XRD and TEM, as well as Raman, FT-IR, and UV−vis spectroscopy.

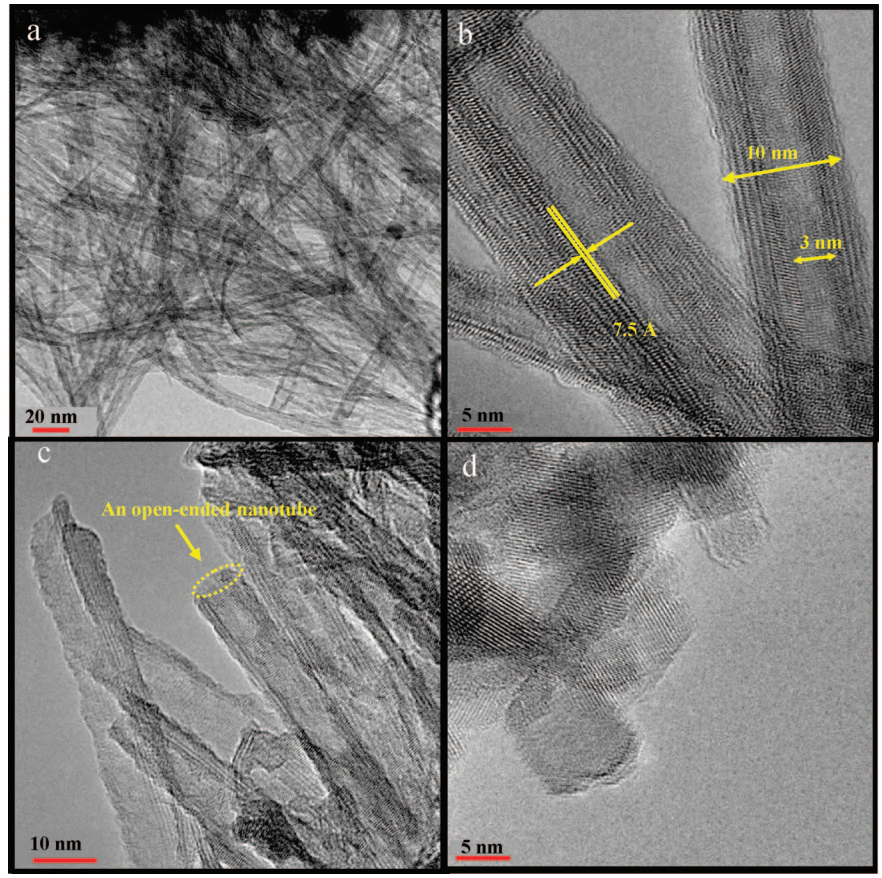

Figure 2. (a) TEM image, (b, c) HRTEM image of TiO_2 nanotubes after annealing at 350 °C, and (d) TEM image of TiO_2 nanotube after annealing at 450 °C.

RESULTS AND DISCUSSION

The XRD patterns of the TNTs were acquired both before and after annealing at 350 °C (Figure 1). From Figure 1a, the as-synthesized TNTs appear to be hydrogen trititanate, which has been proposed to form by scrolling of a nanosheet.[20,21] The diffraction peak near $2\theta = 9.9°$ corresponds to the interlayer spacing of d_{200} in $H_2Ti_3O_7$.[22,23] After annealing at 350 °C, it was found

TABLE 1. Elemental Analysis of PbS/TNTs

sample	concn of thiolactic acid (M)	Pb (wt %)	PbS size (nm)
PbS/TNTs	0.1	21.8	2.4
PbS/TNTs	0.3	22.1	3.6
PbS/TNTs	0.6	24.1	5.6
PbS/TNTs	0.9	29.9	9.4
PbS QDs inside TNTs	0.3	22.7	6.3

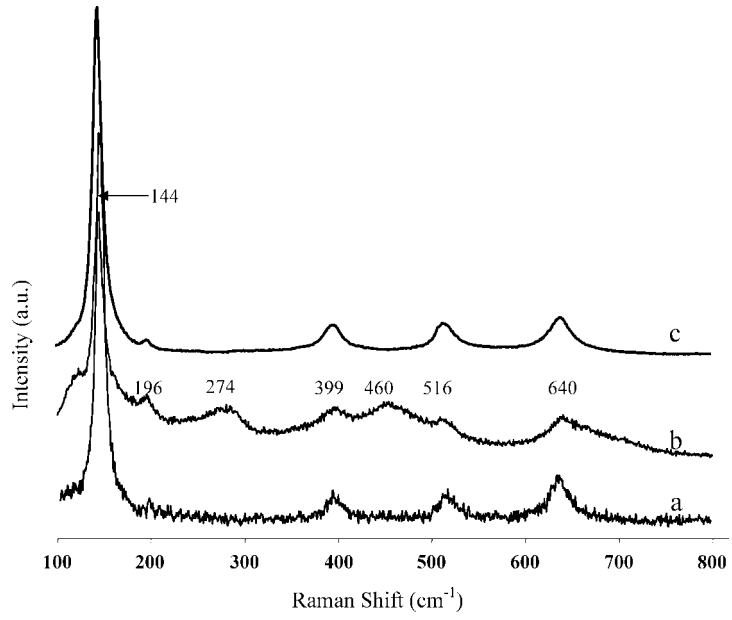

Figure 3. Raman spectra of (a) P25, (b) TNTs annealed at 350 °C, and (c) TNTs annealed at 450 °C.

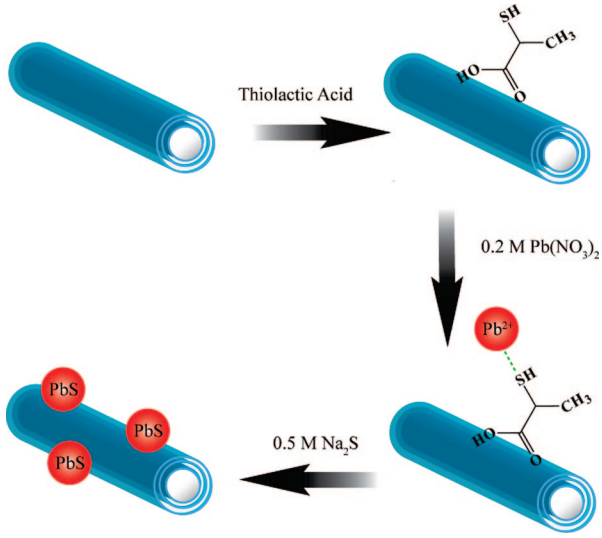

Scheme 1. Preparation of PbS QDs on TiO_2 nanotubes.

that the diffraction peak at $2\theta = 9.9°$ shifted toward a higher angle ($2\theta = 13.3°$), as shown in Figure 1b. The peak shift behavior indicates a decrease in the interlayer space due to dehydration upon heating.[24] It has been reported that the hydrogen trititanate nanotubes can be transformed into the TiO_2 (B) phase and then the anatase phase upon calcination.[25] The peaks at $2\theta = 25.3$, 36.9, and 48.1° indicate the formation of the TiO_2 anatase phase, while the peaks at $2\theta = 13.3$, 29.8, and 43.6° represent the remaining TiO_2 (B) phase. To keep the tubular morphology, the annealing conditions must be strictly controlled (at 350 °C for 75 min). A higher calcination temperature and longer heating times lead to the collapse of lamellar structure of the nanotubes and the transformation of the TiO_2 nanotubes to TiO_2 nanofibers (TNFs) (Figure 2d). The TEM images in Figure 2a,c show open-ended TNTs that are several hundred nanometers in length. The inner and outer diameters of TNTs are 3−5 and 8−10 nm, respectively while the interlayer spacing of the TNTs is around 7.5 Å, as shown in Figure 2b. The BET surface area of the TNTs is 285 m^2/g, which is larger than that of TiO_2 nanorods and particles such as P25 (50 m^2/g).

The Raman spectrum of the TNTs (Figure 3b) also matches with anatase. According to the literature,[26] six Raman active modes, $A_{1g} + 2B_{1g} + 3E_g$, were detected at 144 cm^{-1} (E_g), 197 cm^{-1} (E_g), 399 cm^{-1} (B_{1g}), 513 cm^{-1} (A_{1g}), 519 cm^{-1} (B_{1g}), and 639 cm^{-1}(E_g). The 274 cm^{-1} Raman peak of TNTs appeared after forming the tubular structure and is associated with the Ti−O−H bond resulting from proton exchange with HCl.[27] The peak at 460 cm^{-1} is assigned to the Ti−O bending mode, involving six coordinated oxygen atoms.[28] Compared with P25 and TNFs, the Raman spectra of the TNTs are weaker due to lower crystallinity. TNFs were formed after the collapse of the TNTs upon annealing at high temperature. As shown in Figure 3c, the disappearance of the Ti−OH bond (274 cm^{-1}) is evidence of dehydration. During annealing of the TNTs at high temperature, two Ti−OH bonds condense to form a O−Ti−O bond and a H_2O molecule, resulting in TNFs.[27]

The TNTs were modified with PbS QDs by using a bifunctional thiolactic acid linker. The carboxylic group of thiolactic acid reacts with the surface of TNTs and leaves the thiol group to bind with Pb^{2+}. The growth of PbS nanocrystals occurs after adding a Na_2S solution, as shown in Scheme 1. This experimental design results in PbS QDs attached to the surface of TNTs and prevents the formation of bulk PbS or PbS nanoparticles between TNTs. The size of the PbS QDs can be controlled by adjusting the concentration of thiolactic acid. This is presumably because the amount of lead adsorbed in step 2 of Scheme 1 depends on the amount of linker sites on the TNTs. The TEM images and the corresponding size distribution of the PbS/TNTs samples are shown in Figure 4. When the concentrations of thiolactic acid were 0.1, 0.3, 0.6, and 0.9 M in step 1, the sizes of the resulting PbS QDs were 2, 3−4, 4−5, and 7−9 nm, respectively. The TEM images indicate that PbS QDs were made on both the inside and outside of

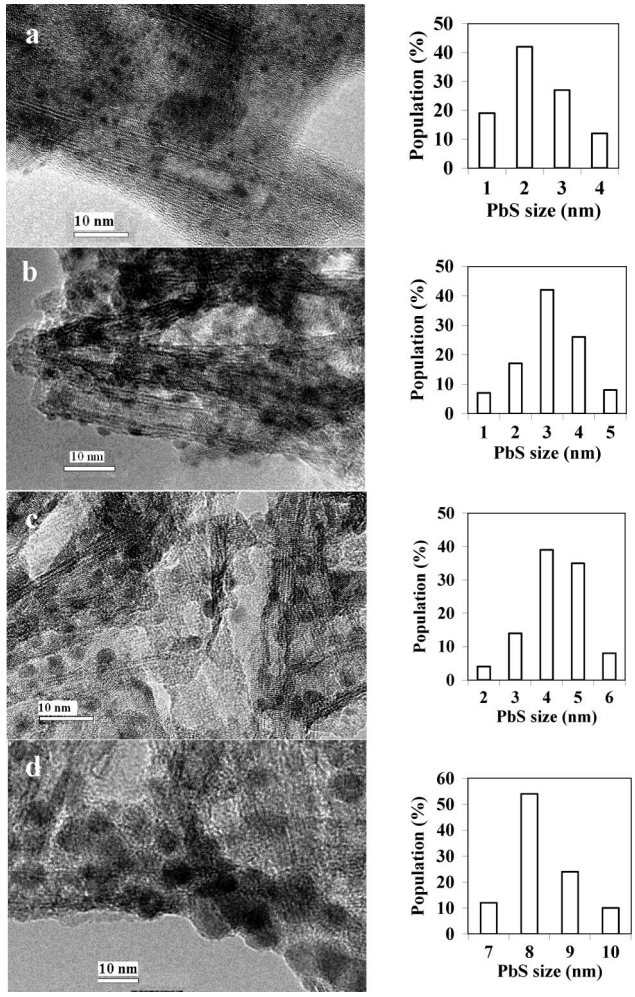

Figure 4. TEM images of PbS/TNTs and the corresponding size distribution of PbS QDs, prepared with different concentrations of thiolactic acid: (a) 0.1 M, (b) 0.3 M, (c) 0.6 M, and (d) 0.9 M.

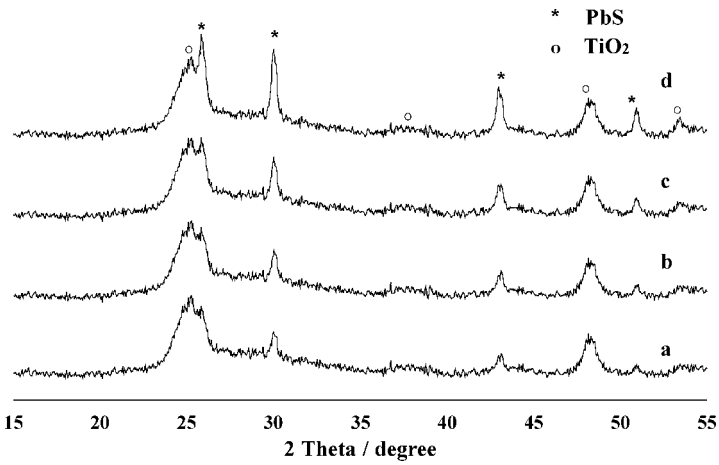

Figure 5. XRD patterns PbS QDs, prepared with different concentrations of thiolactic acid: (a) 0.1 M, (b) 0.3 M, (c) 0.6 M, and (d) 0.9 M.

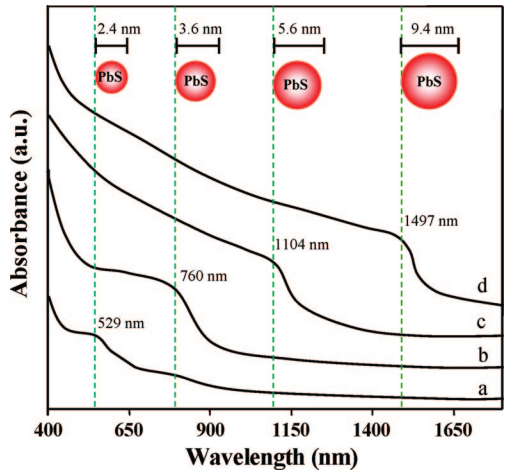

Figure 6. UV−vis absorption spectra of PbS/TiO_2 prepared with different concentration of thiolactic acid: (a) 0.1 M, (b) 0.3 M, (c) 0.6 M, and (d) 0.9 M.

the TiO_2 nanotubes. The XRD patterns of these samples confirmed the presence of the PbS phase as well as the anatase phase of the TNTs (Figure 5). The sizes of the PbS QDs, as calculated by the Scherrer equation, were 2.4, 3.6, 5.6, and 9.4 nm when the concentrations of thiolactic acid were 0.1, 0.3, 0.6, and 0.9 M, respectively (Table 1). This is in close agreement with the TEM results. It is clear that the sizes of the PbS QDs increased when the concentration of thiolactic acid was also increased. The elemental analysis results (Table 1) exhibit a general increase in the wt % of lead as the concentration of thiolactic acid was increased. These results are consistent with the dependence of Pb^{2+} loading on the concentration of thiolactic acid. Therefore, the sizes of the PbS QDs can be controlled by adjusting the concentration of thiolactic acid linkers.

The UV−vis spectra of PbS QDs with different sizes are shown in Figure 6. The absorption peaks are observed at 529, 760, 1104, and 1497 nm when the PbS QDs sizes are 2.4, 3.6, 5.6, and 9.4 nm, respectively. The estimated band gaps of PbS/TNTs samples are 2.34, 1.63, 1.12, and 0.83 eV, which correspond to a wavelength at 529, 760, 1104, and 1497 nm, respectively. The results confirm the band gap size-dependent properties of PbS QDs.

The formation of the PbS/TNTs was followed using FT-IR spectroscopy after each deposition step. The peaks at 1641 and 3382 cm^{-1}, detected in the FT-IR spectrum of the pure TNTs, indicate an interaction between the Ti ions and molecular water. After treatment of the TNTs with a 0.3 M thiolactic acid solution, the carboxylic acid groups interacting with the hydroxyl groups of the TiO_2 surface can be seen in Figure 7b.[19] The peaks at 2568 and 2989 cm^{-1} are the characteristic of $-CH_2-$ and $-SH-$ stretching vibrations, confirming the presence of thiolactic acid. The significant decrease in the peak at 1270 cm^{-1}, the C═O vibration of thiolactic acid, indicates that the thiolactic acid binds to the surface of TNTs using the carboxyl group. As a result, the characteristic vibrations for the carboxylate salt appear at 1550 and 1619 cm^{-1} (CO_2^- asymmetric stretch) and the peaks at 1458 and 1417 cm^{-1} (CO_2^- symmetric stretch).[29] After the addition of Pb^{2+} ions, the interaction between Pb^{2+} and the thiol group leads to a de-

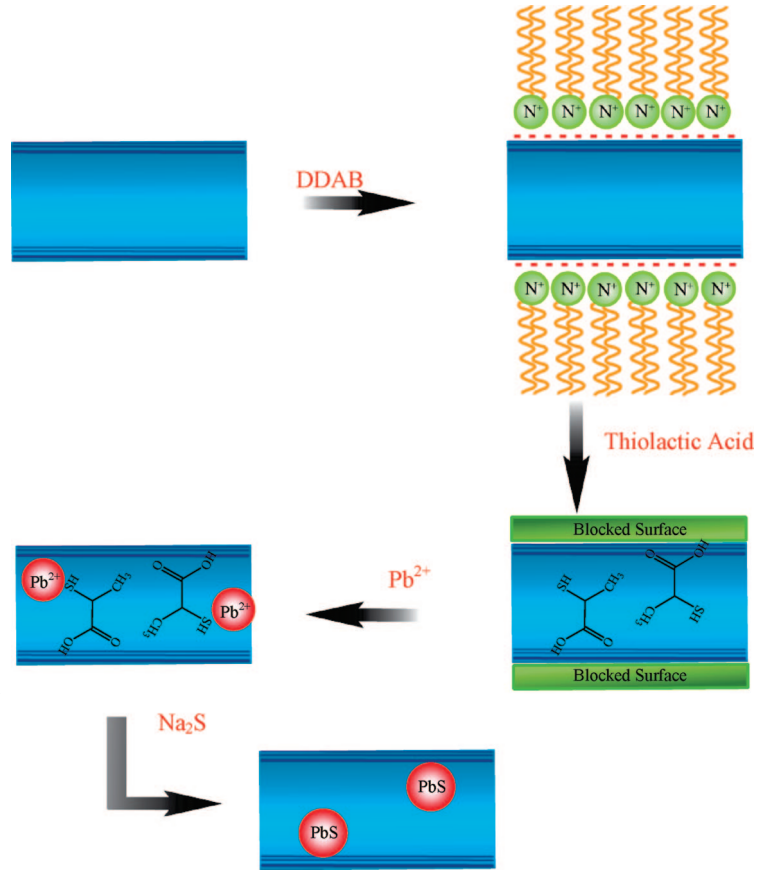

Scheme 2. Deposition of PbS QDs inside TiO_2 nanotubes.

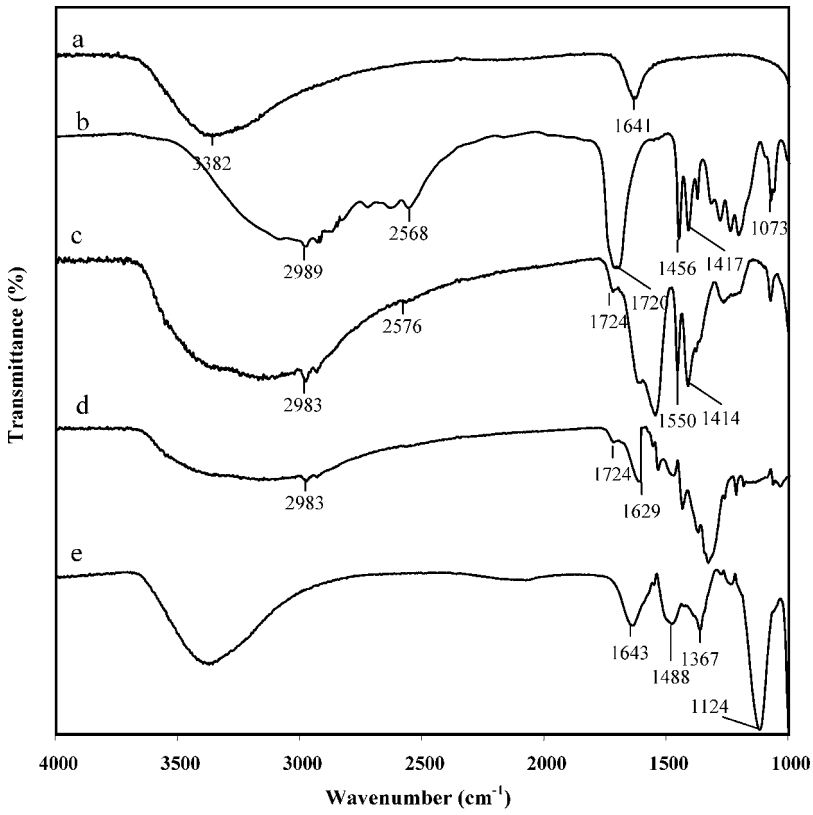

Figure 7. FT-IR spectra of (a) TNTs, (b) thiolactic acid, (c) pretreated TNTs (with thiolactic acid), (d) pretreated TNTs followed by absorption of Pb^{2+}, and (e) PbS/TNTs.

crease in intensity of the stretching vibration for −SH− (2561 cm^{-1}), as shown in Figure 7d.[27] The formation of PbS QDs occurred after adding the Na_2S solution as shown in the XRD patterns (Figure 5). It should be noted that partial oxidation of Na_2S and/or PbS QDs can take place in the presence of O_2. Thus, the peak at 1124 cm^{-1} is likely the S−O stretch of lead thiosulfate.[30–32] However, there is no evidence of crystalline lead sulfate, thiosulfate, or oxide by XRD or TEM. This is not uncommon for PbS QDs and is even observed in commercial samples.

The deposition of PbS QDs only inside the TNTs was achieved by first blocking the outer surface with a surfactant followed by precipitation of PbS, as shown in Scheme 2. The TNTs' surface has a negative charge when placed in an aqueous suspension. As a result, the positively charged molecules can easily absorb onto the surface of TNTs. In order to selectively block the outer surface of TNTs, the $(C_{12}H_{25})_2(CH_3)_2N^+$ surfactant was chosen for two reasons, namely, it has two bulky dodecyl groups to inhibit the absorption inside TNTs, and at the same time, its cationic part helps to attach the negatively charged surface of TNTs. Upon treatment with thiolactic acid, it can only interact with the internal surface of TNTs, yielding the PbS QDs with TNTs. Figure 8 shows TEM images of the PbS/TNTs with a clean external surface of TNTs and PbS QDs located only inside the nanotubes. By blocking the external surface of TNTs, the nanotube surface area, available for thiolactic acid linker, is decreased, meaning that the concentration of thiolactic acid per surface is increased approximately 2-fold compared to that of pure TNTs. With this hypothesis, a result from a 0.3 M thiolactic acid solution should be similar to a result from a 0.6 M thiolactic acid solution if there are no excess thiolactic acid linkers outside the nanotubes. It should be noted from the primary results that the TNTs could absorb the thiolactic acid linkers up to 0.9 M in concentration. Hence, it is possible to absorb all thiolactic acid molecules on the internal surface of TNTs. An average particle size of the PbS QDs calculated by the Scherrer

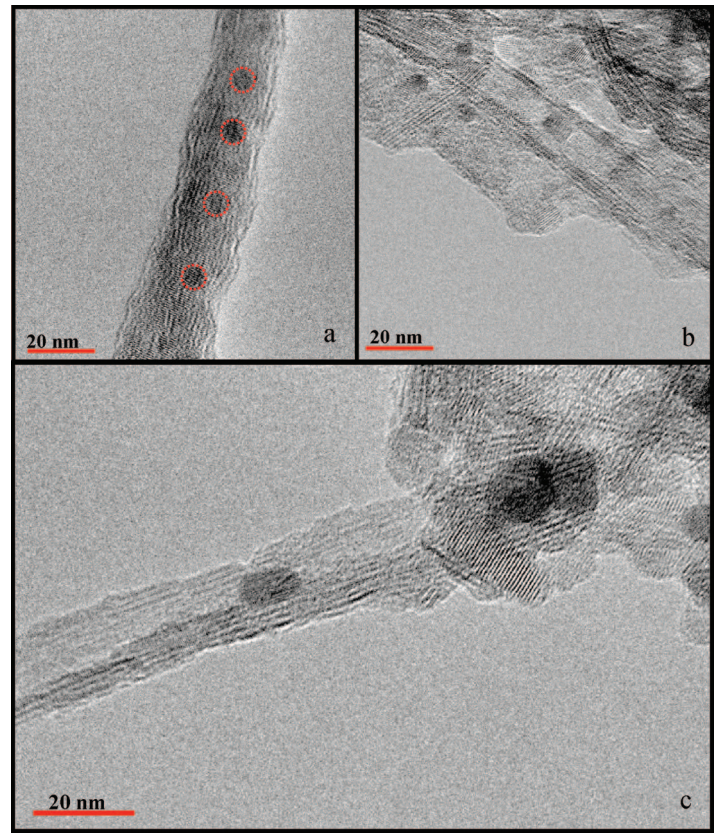

Figure 8. TEM images of PbS/TNTs with PbS QDs inside TNTs, (a and b) the well alignment of PbS QDs inside TNTs, and (c) the capped PbS QDs inside TNTs.

equation is 6.3 nm, which is comparable to the result from a 0.3 M thiolactic acid solution. This is slightly larger than the TNT pore size; however, the shape of PbS QDs formed inside the cavities of the nanotubes changed from a spherical structure to a cylindrical form, as shown in Figure 8c. Moreover, the amount of lead in the samples prepared by 0.3 M thiolactic acid with the blocking method and the regular method matches, as shown in Table 1. It can be concluded that concentration of lead in the sample corresponds to the concentration of thiolactic acid.

The thermostability of PbS/TNTs (QDs inside the nanotubes) was tested by annealing at 500 °C for 1 h in air and Ar atmosphere. After heating in air, the XRD pattern indicates that the PbS QDs were transformed to $PbSO_4$, causing the nanotubes to unscroll as shown by TEM (Figure 9a). The 5−10 nm spheres are $PbSO_4$, while TiO_2 sheets (top right part of image) are visible. In contrast to heating in air, sintering of the PbS nanoparticles occurs upon annealing in an argon atmosphere, yielding PbS nanorods inside the nanotubes (Figure 9b). The length of PbS nanorods, calculated by Scherrer equation, was 25 nm. While the contrast between the TNT and encapsulated PbS nanorod is not clear, the lattice spacings at the core of the TNTs correspond to the 111 (3.43 Å) and 200 (2.95 Å) planes while the nanotube walls match anatase. There is no evidence of either collapsed TiO_2 nanotubes or unscrolled nanotubes, as seen in Figure 9b. This is a surprising result and suggests that the PbS may stabilize the TNTs.

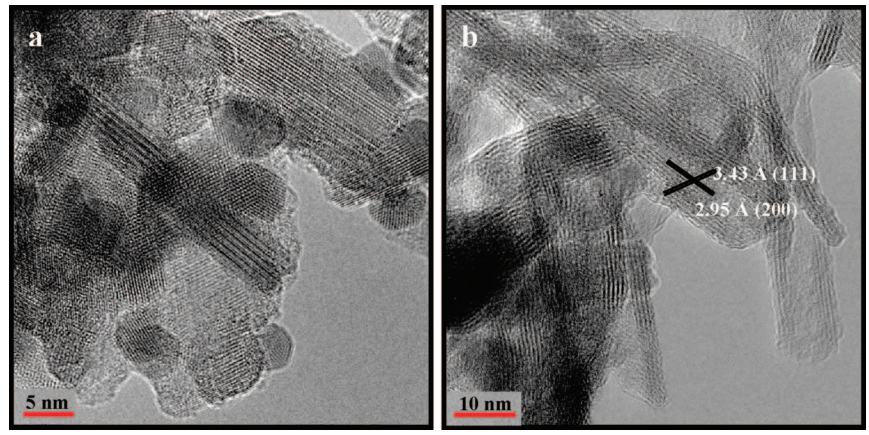

Figure 9. TEM images of TNTs with PbS QDs only on the inside after annealing at 500 °C under (a) air and (b) Ar atmospheres.

CONCLUSION

Anatase TiO_2 nanotubes were obtained from a hydrothermal process of TiO_2 (P25) in the presence of sodium hydroxide followed by an acid wash. Decoration of TiO_2 nanotubes with PbS quantum dots was accomplished by using a thiolactic acid linker to bind Pb^{2+} ions followed by reaction with Na_2S. The PbS QD sizes were controllable with the range of 2−10 nm by adjusting the concentration of thiolactic acid. The selective deposition of PbS QDs only inside TiO_2 nanotubes was carried out using $(C_{12}H_{25})_2(CH_3)_2NBr$ to block the external surface of the nanotubes. Thermal treatment of the encapsulated PbS QDs results in formation of PbS nanorods with retention of the TNT structure. This surprising result could provide a way to fabricate other semiconductor nanorods. Additionally, with the pores of the TNTs filled, the outside surface can be functionalized with other QDs or films. The synthesis of such nanostructures is in progress.

EXPERIMENTAL SECTION

Materials. The Degussa P25 TiO_2 (80% anatase and 20% rutile) was supplied by Degussa Corp. Thiolactic acid (<95%) and sodium sulfide nonahydrate (<98%, ACS reagent) were purchased from Sigma-Aldrich, while lead nitrate (<99%, ACS reagent) was purchased from J. T. Baker. Didodecyldimethylammonium bromide surfactant (99%) was purchased from Alfa Aesar. All chemicals were used without further purification.

Preparation of TNTs. TNTs were synthesized according to literature procedures.[33,34] A mixture of 0.5 g of P25 nanoparticles and 30 mL of a 10 M NaOH aqueous solution was stirred at room temperature for 10 min. The mixture was then transferred to a Teflon-lined autoclave and heated at 150 °C for 24 h. The resulting white precipitate was washed with 0.1 M HCl and water until a pH of 7 was reached, then dried at 90 °C for 10 h followed by annealing at 350 °C for 75 min.

Deposition of PbS QDs onto TNTs. TNTs were pretreated with different concentrations of thiolactic acid (0.1, 0.3, 0.6, and 0.9 M in DI water, pH = 1) for 30 min and then dried at 50 °C for 10 h. A 0.2 M $Pb(NO_3)_2$ aqueous solution was then added into the pretreated TNTs to allow Pb^{2+} ions to absorb on the TNTs surfaces (pH = 3). To crystallize the PbS QDs onto the TNTs, a 0.5 M Na_2S aqueous solution was added, significantly increasing the pH of the solution from 3 to 12. The fabrication process of PbS/TNTs is presented in Scheme 1.

Encapsulation of PbS QDs inside TNTs. To place PbS QDs only on the inside of the TNTs, the nanotubes were first decorated with bulky surfactants. In this experiment, a 0.1 M $(C_{12}H_{25})_2(CH_3)_2NBr$ (DDAB) surfactant aqueous solution was prepared and used as a surface blocking agent. Then 0.25 g of TNTs was stirred with 0.125 g of the surfactant in 25 mL of DI water for 30 min at room temperature The resulting mixture was centrifuged and then dried at 50 °C before adding a 0.3 M thiolactic acid. The surfactant was removed by washing with DI water several times before adding a 0.3 M Pb^{2+} solution followed by precipitating with a 0.5 Na_2S solution. The synthesis process is shown in Scheme 2.

Characterization. X-ray power diffraction (XRD) patterns of the samples were collected using a Scintag XRD 2000 X-ray diffractometer with Cu Kα radiation. The BET surface area of the TNTs was measured on Quantachrome Autosorb I using N_2 adsorption−desorption. Raman spectra were recorded in the region of 100−800 cm^{-1} on a Jobin Yvon Horiba high-resolution LabRam Raman microscope system. A Spectra-Physics model 127 helium−neon laser operating at 35 mW of 633 nm output was the excitation source. The microstructures of TNTs and PbS/TNTs were studied by transmission electron microscopy (TEM)

using a FEI CM200 FEG transmission electron microscope operating at 200 kV. The optical absorption spectra of different sizes were measured from 400 to 1800 nm on a Perkin-Elmer Lambda 900 UV−vis/NIR spectrophotometer. Sample preparation was performed by dispersing a sample in DMF solvent with a concentration of 5 mg mL^{-1} under sonication. The reference solution was 5 mg mL^{-1} TNTs dispersed in DMF solvent. The FT-IR spectra were collected on a Perkin-Elmer spectrum GX FT-IR spectrometer. The FT-IR spectra of samples collected for each fabrication step were obtained using KBr pellets as the sample matrix, while a polyethylene card was used for thiolactic acid. Elemental analysis results were obtained from Galbraith Laboratories, Inc., Knoxville, TN.

Acknowledgment. This work was supported by the Robert A. Welch Foundation and SPRING.

REFERENCES AND NOTES

1. Grätzel, M. J. Dye-Sensitized Solar Cells. *J. Photochem. Photobiol., C* **2003**, *4*, 145–153.
2. Ritterskamp, P.; Kuklya, A.; Wüstkamp, M.-A.; Kerpen, K.; Weidenthaler, C.; Demuth, M. A Titanium Disilicide Derived Semiconducting Catalyst for Water Splitting under Solar Radiation-Reversible Storage of Oxygen and Hydrogen. *Angew. Chem., Int. Ed.* **2007**, *46*, 7770–7774.
3. Nagaveni, K.; Sivalingam, G.; Hegde, M. S.; Madras, G. Photocatalytic Degradation of Organic Compounds Over Combustion-Synthesized Nano-TiO_2. *Environ. Sci. Technol.* **2004**, *38*, 1600–1604.
4. Weller, H. Quantized Semiconductor Particles: A Novel State of Matter for Materials Science. *Adv. Mater.* **1993**, *5*, 88–95.
5. Peterson, J. J.; Krauss, T. D. Fluorescence Spectroscopy of Single Lead Sulfide Quantum Dots. *Nano Lett.* **2006**, *6*, 510–514.
6. Ellingson, R. J.; Beard, M. C.; Johnson, J. C.; Yu, P.; Micic, O. I.; Nozik, A. J.; Shabaev, A.; Efros, A. L. Highly Efficient Multiple Exciton Generation in Colloidal PbSe and PbS Quantum Dots. *Nano Lett.* **2005**, *5*, 865–871.
7. Nozik, A. J. Exciton Multiplication and Relaxation Dynamics in Quantum Dots: Applications to Ultrahigh-Efficiency Solar Photon Conversion. *Inorg. Chem.* **2005**, *44*, 6893–6899.
8. Wang, P.; Wang, L.; Ma, B.; Li, B.; Qui, Y. TiO_2 Surface Modification and Characterization with Nanosized PbS in Dye-Sensitized Solar Cells. *J. Phys. Chem. B* **2006**, *110*, 14406–14409.
9. Nenadovic, M. T.; Comor, M. I.; Vasic, V.; Micic, O. I. Transient Bleaching of Small PbS Colloids. Influence of Surface Properties. *J. Phys. Chem.* **1990**, *94*, 6390–6396.
10. Liveri, V. T.; Rosi, M.; D'Arrigo, G.; Manno, D.; Micocci, G. Synthesis and Characterization of ZnS Nanoparticles in Water/AOT/*n*-heptane Microemulsions. *Appl. Phys. A: Mater. Sci. Process.* **1999**, *69*, 369–373.
11. Moffitt, M.; Eisenberg, A. Size Control of Nanoparticles in Semiconductor-Polymer Composites. 1. Control via Multiplet Aggregation Numbers in Styrene-Based Random Ionomers. *Chem. Mater.* **1995**, *7*, 1178–1184.
12. Tasson, R.; Schrock, R. R. Synthesis of PbS Nanoclusters within Microphase-Separated Diblock Copolymer Films. *Chem. Mater.* **1994**, *6*, 744–749.
13. Kane, R. S.; Cohen, R. E.; Silbery, R. Synthesis of PbS Nanoclusters within Block Copolymer Nanoreactors. *Chem. Mater.* **1996**, *8*, 1919–1924.
14. Hoyer, P.; Könenkamp, R. Photoconduction in Porous TiO_2 Sensitized by PbS Quantum Dots. *Appl. Phys. Lett.* **1995**, *66*, 349–351.
15. Sun, Y.; Hao, E.; Zhang, X.; Yang, B.; Shen, J.; Chi, L.; Fuchs, H. Buildup of Composite Films Containing TiO_2/PbS Nanoparticles and Polyelectrolytes Based on Electrostatic Interaction. *Langmuir* **1997**, *13*, 5168–5174.
16. Yang, S.-M.; Huang, C.-H.; Zhai, J.; Wang, Z.-S.; Jiang, L. High Photostability and Quantum Yield of Nanoporous TiO_2 Thin Film Electrodes Co-Sensitized with Capped Sulfides. *J. Mater. Chem.* **2002**, *12*, 1459–1464.
17. Plass, R.; Pelet, S.; Krueger, J.; Grätzel, M. Quantum Dot Sensitization of Organic-Inorganic Hybrid Solar Cells. *J. Phys. Chem. B* **2002**, *106*, 7578–7580.
18. Sun, W.-T.; Yu, Y.; Pan, H.-Y.; Gao, X.-F.; Chen, Q.; Peng, L.-M. CdS Quantum Dots Sensitized TiO_2 Nanotube-Array Photoelectrodes. *J. Am. Chem. Soc.* **2008**, *130*, 1124–1125.
19. Kim, J. C.; Choi, J.; Lee, Y. B.; Hong, J. H.; Lee, J. I.; Yang, J. W.; Lee, W. I.; Hur, N. H. Enhanced Photocatalytic Activity in Composites of TiO_2 Nanotubes and CdS Nanoparticles. *Chem. Commun.* **2006**, *48*, 5024–5026.
20. Zhang, S.; Peng, L.-M.; Chen, Q.; Du, G. H; Dawson, G.; Zhou, W. Z. Formation Mechanism of $H_2Ti_3O_7$ Nanotubes. *Phys. Rev. Lett.* **2003**, *91*, 256103.
21. Zhang, S.; Chen, Q.; Peng, L.-M. Structure and Formation of $H_2Ti_3O_7$ Nanotubes in an Alkali Environment. *Phys. Rev. B* **2005**, *71*, 014104.
22. Chen, Q.; Du, G. H.; Zhang, S.; Peng, L. M. The Structure of Trititanate Nanotubes. *Acta Crystallogr., Sect. B* **2002**, *58*, 587–593.
23. Chen, Q.; Zhou, W.; Du, G.; Peng, L.-M. Trititanate Nanotubes Made *via* a Single Alkali Treatment. *Adv. Mater.* **2002**, *14*, 1208–1211.
24. Suzuki, Y.; Yoshikawa, S. Synthesis and Thermal Analyses of TiO_2-Derived Nanotubes Prepared by the Hydrothermal Method. *J. Mater. Res.* **2004**, *19*, 982–985.
25. Morgado, E.; Jardim, P. M.; Marinkovic, B. A.; Rizzo, F. C; Abreu, M.; Zotin, J. L.; Araujo, A. S. Multistep Structural Transition of Hydrogen Trititanate Nanotubes into TiO_2-B Nanotubes: A Comparison Study between Nanostructred and Bulk Materials. *Nanotechnology* **2007**, *18*, 495710.
26. Mikami, M; Arakanura, S.; Kitao, O.; Arakwa, H. Lattice Dynamics and Dielectric Properties of TiO_2 Anatase: A First-Principles Study. *Phys. Rev. B* **2002**, *66*, 155213–155216.
27. Qian, L.; Du, Z.-L.; Yang, S.-Y.; Jin, Z.-S. Raman Study of Titania Nanotube by Soft Chemical Process. *J. Mol. Struct.* **2005**, *749*, 103–107.
28. Kasuga, T.; Hiramatsu, M.; Hoson, A.; Sekino, T.; Niihara, K. Titania Nanotubes Prepared by Chemical Processing. *Adv. Mater.* **1999**, *11*, 1307–1311.
29. Rajh, T.; Ostafin, A. E.; Micic, O. I.; Tiede, D. M.; Thurnauer, M. C. Surface Modification of Small Particle TiO_2 Colloids with Cysteine for Enhancd Photochemical Reduction: An EPR Study. *J. Phys. Chem.* **1996**, *100*, 4538–4545.
30. Chernyshova, I. V. Anodic Processes on a Galena (PbS) Electrode in the Presence of *n*-Butyl Xanthate Studied FTIR-Spectroelectrochemically. *J. Phys. Chem. B* **2001**, *105*, 8185–8191.
31. Chernyshova, I. V.; Andreev, S. I. Spectroscopic Study of Galena Surface Oxidation in Aqueous Solutions: I. Identification of Surface Species by XPS and ATR/FTIR Spectroscopy. *Appl. Surf. Sci.* **1997**, *108*, 225–236.
32. Kilsa, K.; Mayo, E. I.; Brunschwig, B. S.; Gray, H. B.; Lewis, N. S.; Winkler, J. R. Anchoring Group and Auxiliary Ligand Effects on the Binding of Ruthenium Complexes to Nanocrystalline TiO_2 Photoelectrodes. *J. Phys. Chem. B* **2004**, *108*, 15640–15651.
33. Du, G. H.; Chen, Q.; Che, R. C.; Yuan, Z. Y.; Peng, L. M. Preparation and Structure Analysis of Titanium Oxide Nanotubes. *Appl. Phys. Lett.* **2001**, *79*, 3702–3704.
34. Khan, M. A.; Jung, H.-T.; Yang, O.-B. Synthesis and Characterization of Ultrahigh Crystalline TiO_2 Nanotubes. *J. Phys. Chem. B* **2006**, *110*, 6626–6630.